down to 30°C at a cooling rate of 10°C/min. The heat of fusion is calculated by integrating the area under the DSC endothermic peak for the first time. The degree of crystallinity of UHMWPE specimen was calculated by normalizing the heat of melting to that of 100% crystalline PE, by the following equation [20,21]:

$$X_C(\%) = \frac{\Delta H_m}{\Delta H_m^{100}} \times 100 \quad (1)$$

where $X_C$ is the degree of crystallinity, $\Delta H_m$ is the heat of fusion corrected for one gram of UHMWPE specimen, $\Delta H_m^{100}$ is the heat of fusion for 100% crystalline UHMWPE taken as 290 J/g.

2.3. Multi-directional pin-on-plate wear test

Similar to the DSC tests, three distinct regions were selected to perform the wear tests. The testing samples were machined to a proper shape for the wear tests by using the lathe. The geometry of the test specimen is shown in Fig. 1. The parameters (a, b, c) used for the processing at different regions are based on the results of oxidation behavior of the cross-section measured by FTIR mapping method and shown in Table 1. Before the wear tests, the average OI and micro-hardness of the testing surfaces were measured by FTIR and micro-indentation.

The wear behavior of shelf-aged specimen was evaluated by using a three-station multi-directional sliding pin-on-plate wear tester in which the fixed pin specimen articulates upon the plate specimen surface along a circular path with a diameter of 30 mm [22]. Medical grade cast CoCrMo alloy was used as a plate specimen and polished by using diamond slurry to a surface roughness $R_a$ of 0.01±0.005 μm measured by a stylus roughness meter. Prior to the wear test, both the pin and plate specimens were ultrasonically cleaned in distilled water with a detergent (polyoxyethylene p-t-octylphenylether) for 30 min. Then the specimens were rinsed with a stream of distilled water to remove the detergent and ultrasonically washed again for 30 min with distilled water. Finally, the specimens were washed ultrasonically in ethanol for 15 min and then dried in a vacuum desiccator for 2 h at room temperature.

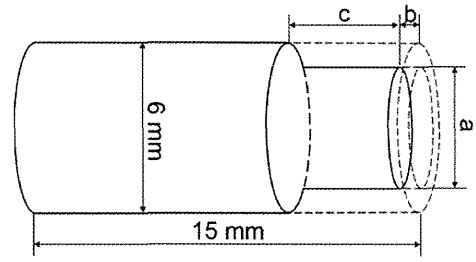


Fig. 1 The geometry of pin specimen

Wear tests were carried out under the lubrication of 30% bovine serum solution at room temperature. A mean contact pressure of 6 MPa and a sliding velocity of 50 mm/s were applied. All experiments were stopped after 10 km sliding distance. The wear amount of the pin specimen was determined from the weight loss. At an interval of 5 km sliding distance, the pin specimen was removed from the test apparatus and cleaned by the same procedure described before. Then the specimen was weighed to an accuracy of 0.01 mg. A static control pin was soaked in the same lubricant to estimate the weight gain due to the fluid uptake from the lubricant. Then, the specific wear rate $k$ ($mm^3N^{-1}m^{-1}$) was calculated by dividing the wear volume $\Delta V$ ($mm^3$) by the sliding distance $S$ (m) and applied normal load $F$ (N) to characterize the wear resistance of the UHMWPE pin specimens. Non-crosslinked UHMWPE without shelf-ageing was used as control.

2.4. Morphology observation

The morphologies of worn surfaces were observed with an optical microscope (Nikon Eclipse LV 150) in bright field and scanning electron microscope (SEM, JEOL JCM-6000). Prior to the SEM observation, the samples were coated with a ~5 nm-thick platinum layer to prevent them from charging. The samples were imaged using secondary electrons at an accelerating voltage of 15 kV.

Table 1 The parameters (a, b, c) of the processing

| Material | Regions | Parameter a / (mm) | Parameter b / (mm) | Parameter c / (mm) |
|---|---|---|---|---|
| Non-crosslinked UHMWPE | surface | 6.0 | 0.0 | 0.0 |
| Shelf-aged 50 kGy UHMWPE | surface | 4.0 | 0.0 | 3.0 |
| Shelf-aged 50 kGy UHMWPE | subsurface | 3.8 | 1.1 | 3.0 |
| Shelf-aged 50 kGy UHMWPE | center | 2.8 | 7.5 | 3.0 |
| Shelf-aged 100 kGy UHMWPE | surface | 4.0 | 0.0 | 3.0 |
| Shelf-aged 100 kGy UHMWPE | subsurface | 3.8 | 1.0 | 3.0 |
| Shelf-aged 100 kGy UHMWPE | center | 2.8 | 7.5 | 3.0 |

## 3. Results

Fig. 2 shows the line-scan ATR spectra collected along the radial direction of the cross-section of the testing samples. Compared with non-irradiated UHMWPE (Fig. 2(a)), the crosslinked UHMWPE spectra (Figs. 2(b), (c)) showed the clear absorptions of acids at 1712 $cm^{-1}$ with shoulder absorptions of esters at 1740 $cm^{-1}$ which can be attributed to C-O stretching. No significant differences were observed between 50 kGy and 100 kGy ATR spectra. The largest absorption intensity of carbonyl groups around 1720 $cm^{-1}$ is at the subsurface for both shelf-aged samples. Along the cross-section, the inhomogeneous presence of acids indicated a depth-dependent oxidation phenomenon of shelf-aged crosslinked UHWMPE.

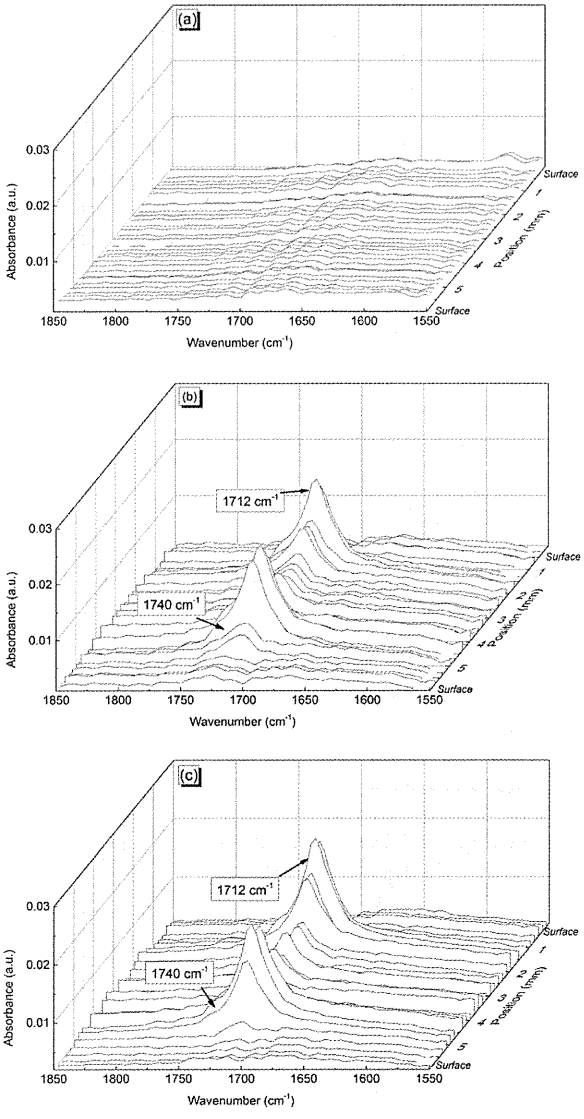


Fig. 2 ATR spectra collected along radial direction of cross-section of non-crosslinked (a), 50 kGy (b) and 100 kGy (c) crosslinked UHMWPE

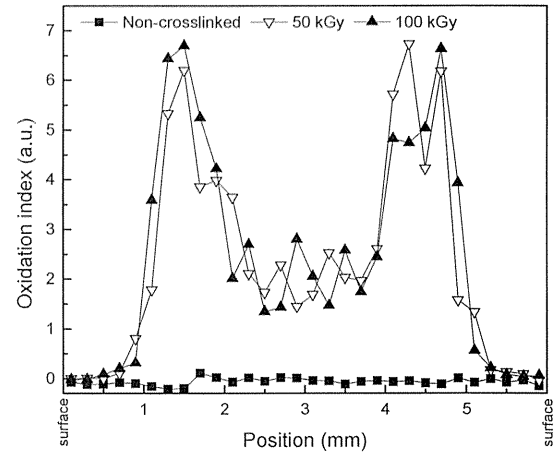


Fig. 3 Oxidation index as a function of position of non-crosslinked and crosslinked UHMWPE

The oxidation index (OI) of testing samples are calculated and plotted against position along the radial direction of the cross-section in Fig. 3. The OI of the non-crosslinked sample showed a relatively low and stable trend through the whole cross-section. Both of the two dose level crosslinked UHMWPE were susceptible to oxidation and showed the similar oxidation index profiles varying with the position after 7-year shelf-ageing. The maximum values of OI for 50 kGy and 100 kGy samples were 6.62 and 6.66, respectively and obtained at around 1.5 mm below the surface. The OI measured close to the surface showed relatively low values in the crosslinked samples, even comparing with the non-crosslinked sample. In addition, as the measurement location near the center, the OI of crosslinked UHMWPEs decreased and showed relatively fluctuant values at center region.

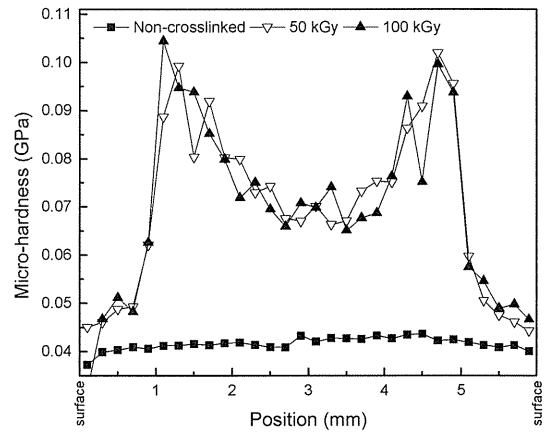


Fig. 4 Micro-hardness as a function of position of non-crosslinked and crosslinked UHMWPE

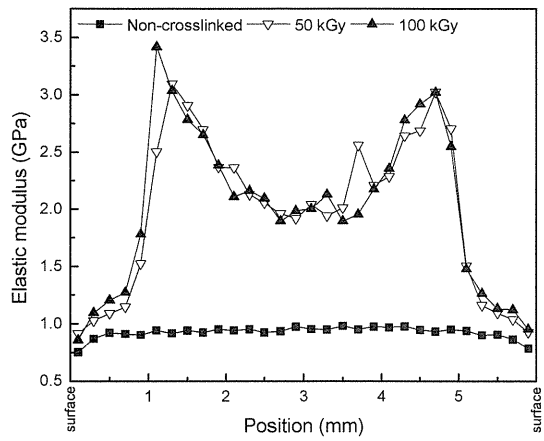


Fig. 5 Elastic modulus as a function of position of non-crosslinked and crosslinked UHMWPE

The micro-indentation test results of non-crosslinked and crosslinked UHMWPE are shown in Fig. 4 and Fig. 5. The profiles of micro-hardness and elastic modulus followed the similar trend as the oxidation index profile and indicated that oxidation behavior had a direct impact on the mechanical properties of shelf-aged crosslinked material. In addition, the two dose levels crosslinked UHMWPEs had the similar maximum value of micro-hardness, which is around 0.10 GPa and elastic modulus, which is around 3.14 GPa. The position of the peaks along the cross-section was at around 1.4 mm below the surface. No significant differences were found between the two shelf-aged crosslinked UHMWPEs.

The average values of OI, micro-hardness and crystallinity for all the testing surfaces measured before the wear tests are shown in Fig. 6 together with the results of the wear tests. Compared with the non-crosslinked sample, the OI, micro-hardness and crystallinity of crosslinked UHMWPE were all higher at the surface regions after 7-year shelf-ageing. The average values of OI, micro-hardness and crystallinity of 50 kGy sample were lower than 100 kGy sample at subsurface and center regions, while different patterns were observed in micro-hardness and crystallinity at surface region.

The specific wear rates at selected regions of non-crosslinked and crosslinked UHMWPE are shown in Fig. 6(d). The results showed that the specific wear rates at high-oxidized regions (subsurface and center region) were two orders of magnitude higher than at the surface regions for crosslinked UHMWPE. Compared with the non-crosslinked sample, the crosslinked samples still maintained excellent wear resistance after 7-year shelf-ageing at the surface region. The specific wear rates of 50 kGy and 100 kGy samples at the surface region were $9.57\times10^{-8}$ and $3.19\times10^{-8}$ $mm^3/(Nm)$ which is about one third and one tenth of the non-crosslinked sample ($3.01\times10^{-7}$ $mm^3/(Nm)$), respectively. Moreover, the specific wear rates at subsurface regions and center regions followed the similar trend as the oxidation index,

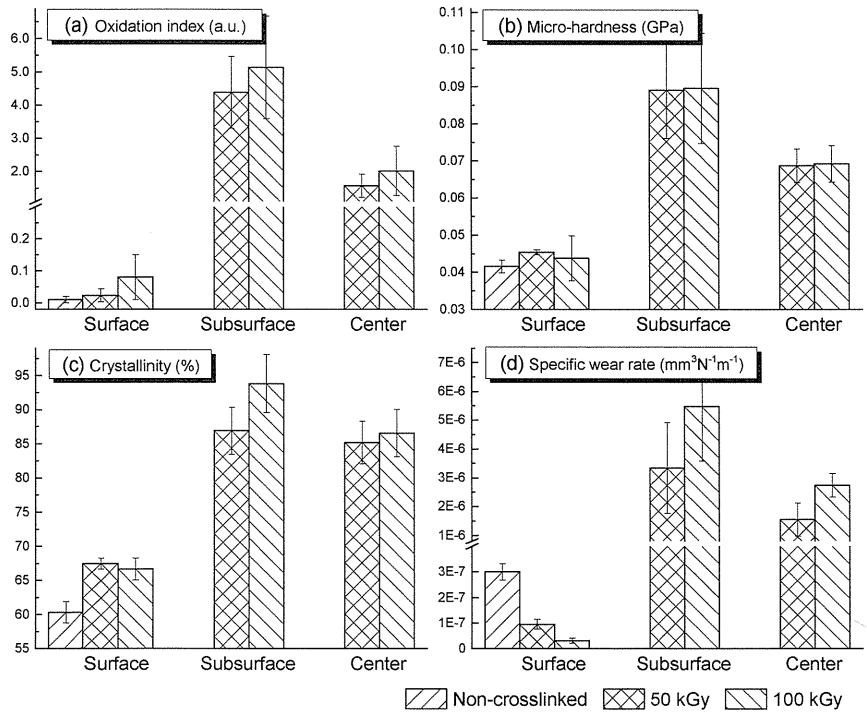


Fig. 6 The OI (a), micro-hardness (b), crystallinity (c) and specific wear rate (d) at the selected testing surfaces of non-crosslinked and crosslinked UHMWPE (mean ± SD, $n$=3)

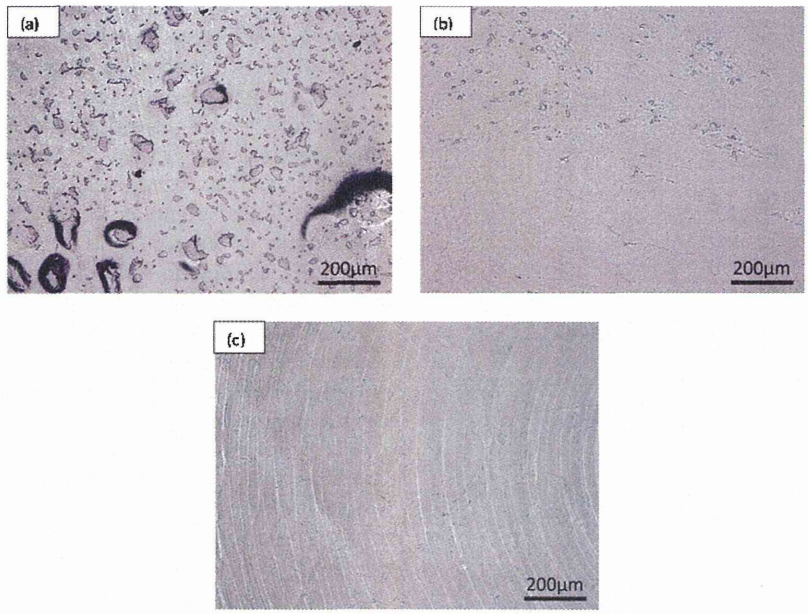


Fig. 7 Appearance of non-crosslinked (a), 50 kGy (b) and 100 kGy (c) worn surfaces at the surface region

micro-hardness and crystallinity.

Fig. 7 shows the morphological characteristics of the UHMWPE worn surfaces at the surface region after the multi-directional sliding tests, observed by optical microscopy. The appearance of the worn surfaces was significantly different between each specimen. No machining marks were observed on the worn morphology of non-crosslinked sample (Fig. 7(a)), but amount of debris and sporadic protuberance were observed. Slight machining marks and a small quantity of debris were the main features of the worn morphology of the 50 kGy sample as shown in Fig. 7(b), while obvious machining marks were observed on the worn surface of the 100 kGy sample (Fig. 7(c)). Morphology observation results were consistent with the results of wear rate.

The fine structure of the worn surface was also examined with the scanning electron microscope (SEM).

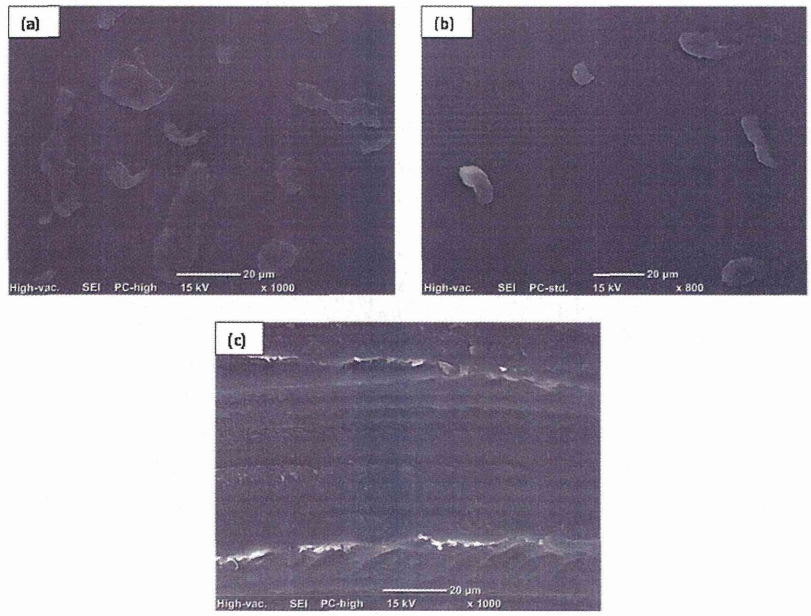


Fig. 8 SEM images of non-crosslinked (a), 50 kGy (b) and 100 kGy (c) worn surfaces at the surface region

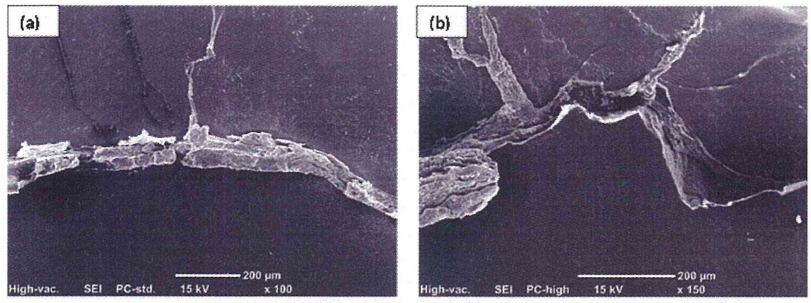


Fig. 9 SEM images of 50 kGy (a) and 100 kGy (b) worn surfaces at the subsurface region

SEM images of worn surfaces at the surface region are shown in Fig. 8. Similar features were observed with the optical microscopy. However, no machining marks were observed on the 50 kGy sample, and the 5 nm-thick platinum coating layer was probably responsible for it. Fig. 9 shows the SEM images of the worn surface at the subsurface region of crosslinked samples. Cracks, fracture and fibril formations were observed on both crosslinked UHMWPE worn surfaces. Compared with the 50 kGy sample (Fig. 9(a)), more cracks and fracture occurred on the 100 kGy sample (Fig. 9(b)), and this may reflect the more serious wear rate of the 100 kGy sample at the subsurface region, which is consistent with the wear rate results (Fig. 6(d)). Furthermore, similar features of masses of fibril formations were observed at the center region of the worn surfaces for both crosslinked samples as shown in Fig. 10.

## 4. Discussion

Although the link between the oxidation behavior and mechanical properties of crosslinked UHMWPE has been investigated by many studies [18,23], the relationship between the wear rate and oxidation behavior remains unclear.

The results of this study agreed with earlier investigations [13,18,23] that showed the depth-dependent oxidation behavior of crosslinked UHMWPE shelf-aged after gamma-irradiation in air. The results also showed that the profiles of micro-hardness (Fig. 4) and modulus (Fig. 5) along the cross-section of crosslinked samples mirrored the OI profile (Fig. 3). It indicated that the effect of oxidation on the mechanical properties of shelf-aged crosslinked UHMWPE was strong and direct. The maximum value of OI, micro-hardness and elastic modulus of gamma-irradiated UHMWPE occurred at the subsurface (Figs. 2-5). The highly oxidized subsurface region was recognized as a circular band with a distinctive white color in the microtomed slices as shown in Fig. 11 and usually called "white band" [24]. The embrittled subsurface white band is susceptible to cracking and delamination, which would be the critical element to cause early failures of the artificial joint.

The correlation between the wear rate and oxidation index was shown in Fig. 12. The figure indicated that the wear rate of the crosslinked UHMWPE was significantly increased with increasing OI. Worn surface morphology observation showed that the surface regions of shelf-aged samples (Fig. 7) still have some machining marks. However, the subsurface regions of shelf-aged samples (Fig. 9) showed fracture, cracks and more severe wear patterns and the machining marks totally disappeared. The center regions showed moderate wear patterns; the removal of machining marks and formation of many

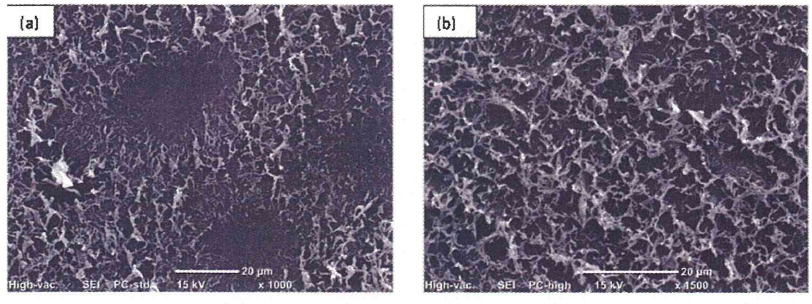


Fig. 10 SEM images of 50 kGy (a) and 100 kGy (b) worn surfaces at the center region

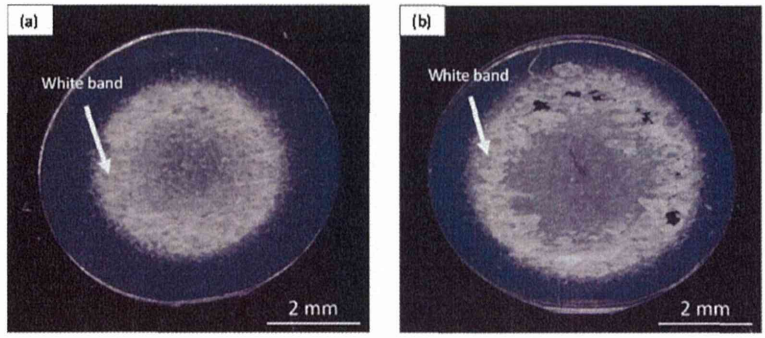


Fig. 11 Optical micrographs of microtomed 50 kGy (a) and 100 kGy (b) UHMWPE slices

fibrils without cracks and fractures. Therefore, the characteristics in the worn surface morphology of each region coincided with the evaluated specific wear rate and both values certainly related to the OI.

How could the higher oxidation result in the degradation of wear resistance in the gamma-irradiated UHMWPE. Gamma radiation is supposed to form the UHMWPE crosslinks to improve the wear-resistance of this polymer [6]. However, gamma irradiation of polyethylene components, which dissociates molecular bonds, not only leads to crosslinking but also induces the formation of residual free radicals [9,12]. The reaction between residual free radicals and diffused oxygen molecules initiates a significant concentration of peroxy radicals to start the oxidative degradation in UHMWPE. With ageing, oxygen diffuses deep into the UHMWPE components, reacts with the free radicals and eventually causes more oxidation. This process results in a higher oxidation index and lower molecular weight at the subsurface. The shortened molecular chains enhance the chain mobility and provide more chance of recrystallization by crystal perfection processes, thus the degree of crystallinity of UHMWPE increases following oxidation (Fig. 6(c)). Consequently, the mechanical properties, such as micro-hardness and elastic modulus, increased since they are depended on the crystallinity in many kinds of polymers (Fig. 6(b)). Meanwhile, the shortened molecular chains also reduce the abrasion resistance of polymer materials due to the reduction of the molecular weight, which is an important factor increasing the strength and wear resistance of polymers. In addition, recrystallization process, which was caused by the oxidation, results in polymer shrinkage in the same volume [24]. This phenomenon will cause a rough, brittle and porous microstructure (Fig. 11) in the material. Such a deteriorated microstructure is supposed to be the main reason for the highest wear rate at the most oxidized subsurface region.

Interestingly, Fig. 12 showed that the slope of the graph increased as the radiation dose increased. Researchers [11,13] pointed out that the radiation dose has a certain effect on the oxidation and mechanical properties of crosslinked UHMWPE, due to the difference in the crosslink density induced by the different dose level of gamma irradiation. Thus, the crosslink density may play a certain role in the dose dependent wear behavior of gamma-irradiated UHMWPE confirmed in our multidirectional wear tests.

In our present work, at surface region with the lowest OI values, the specific wear rate of UHMWPE decreased with increasing the radiation dose. In general with increasing radiation dose, there is an increase in crosslink density. The 100 kGy sample with higher crosslinked density could therefore enjoy a lower wear rate at the surface region. The morphologies at the surface region are also suggesting significant effects of the radiation dose on the wear mechanism of UHMWPE. Amount of debris and sporadic protuberances were all imaged at the worn surface of non-crosslinked sample (Fig. 7(a) and Fig. 8(a)). Less or lightly these features were observed on the 50 kGy worn surface (Fig. 7(b) and Fig. 8(b)). All these features are related to the adhesive wear

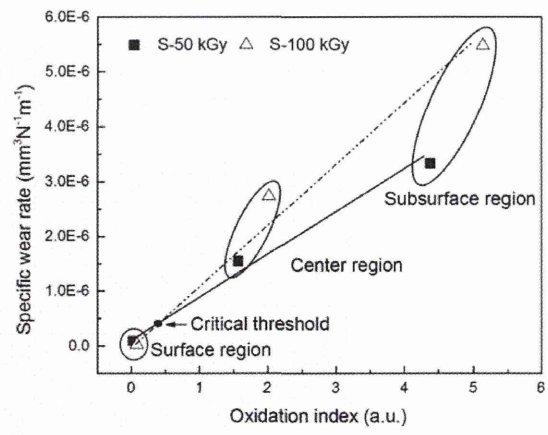


Fig. 12 The relationship between the specific wear rate and oxidation index of crosslinked UHMWPE

mechanisms associated with a certain amount of plastic deformation. On the other hand, the worn surface of 100 kGy sample (Fig. 7(c) and Fig. 8(c)) had the distinct machine marks attached with some fine wear debris. Surface cracks related to fatigue mechanisms were also found. However, the fibrillated wear particles and protuberances generated by the adhesive wear process were hardly observed. The increased number of chemical bonds between adjacent molecular chains formed by the increased crosslink density can retard the chain mobility and enhance the molecular resistance against shear rupture. Consequently, increased radiation dose enhanced the resistance to the adhesive wear and had a predominant impact on the wear behavior of UHMWPE.

Although the effects of the crosslink density on the oxidation, mechanical and wear properties of crosslinked UHMWPE were not clear, the wear mechanism seemed to be mainly dependent on the oxidation behavior when the OI is greater than a certain "critical threshold" (Fig. 12). Similar features of masses of fibril formations on the wear surfaces were observed on both crosslinked samples at the center region as shown in Fig. 10. Fractures, cracks, fiber drawing and scratches, which indicated a mixed wear mechanism including abrasive wear and fatigue, are the main wear characteristics observed on the more oxidized subsurface regions for both crosslinked UHMWPEs (Fig. 9). It seems that more severe fractures were founded at the subsurface of 100 kGy sample, which is related to the higher OI and higher wear rate compared with the 50 kGy sample.

A limitation of this study was that the region of each sample for the wear test was not a continuous variable. Only three regions of each sample were analyzed, thus, there was insufficient data to accurately quantify the relationship between the OI, radiation dose and wear rate. In order to clarify the radiation dose and OI effects and determine a "critical threshold", more regions with different oxidation conditions of two shelf-aged gamma-irradiated UHMWPEs should be tested.

## 5. Conclusions

Oxidation behavior and its effects on the mechanical and wear properties of crosslinked UHMWPE after 7-year shelf-ageing were investigated in this paper. It was shown that the micro-hardness, elastic modulus and crystallinity increased with the increase of the oxidation index, while the wear resistance decreased. The wear analysis may indicate that, when the OI is under a critical threshold, the crosslink density is the main cause of the difference of wear mechanisms; and above the critical threshold, the oxidation will have an important effect on the wear behavior of crosslinked UHMWPE. However, more evidence is needed to confirm this hypothesis.

## Reference

[1] Schwartz, C. J., Bahadur, S. and Mallapragada, S. K., "Effect of Crosslinking and Pt–Zr Quasicrystal Fillers on the Mechanical Properties and Wear Resistance of UHMWPE for Use in Artificial Joints," Wear, 263, 7-12, 2007, 1072-1080.

[2] Ge, S., Wang, S. and Huang, X., "Increasing the Wear Resistance of UHMWPE Acetabular Cups by Adding Natural Biocompatible Particles," Wear, 267, 5-8, 2009, 770-776.

[3] Shi, X., Wang, Q., Xu, L., Ge, S. and Wang, C., "Hydrogenated Diamond-Like Carbon Film Deposited on UHMWPE by RF-PECVD," Applied Surface Science, 255, 19, 2009, 8246-8251.

[4] Sobieraj, M. C. and Rimnac, C. M., "Ultra High Molecular Weight Polyethylene: Mechanics, Morphology, and Clinical Behavior," Journal of the Mechanical Behavior of Biomedical Materials, 2, 5, 2009, 433-443.

[5] Atwood, S. A., Citters, D. W., Patten, E. W., Furmanski, J., Ries, M. D. and Pruitt, L. A., "Tradeoffs Amongst Fatigue, Wear, and Oxidation Resistance of Cross-Linked Ultra-High Molecular Weight Polyethylene," Journal of the Mechanical Behavior of Biomedical Materials, 4, 7, 2011, 1033-1045.

[6] Muratoglu, O. K., Bragdon, C. R., O'Connor, D. O., Jasty, M., Harris, W. H., Gul, R. and McGarry F., "Unified Wear Model for Highly Crosslinked Ultra-High Molecular Weight Polyethylenes (UHMWPE)," Biomaterials, 20, 16, 1999, 1463-1470.

[7] Naidu, S. H., Bixler, B. L. and Moulton, M. J., "Radiation-Induced Physical Changes in UHMWPE Implant Components," Orthopedics, 20, 2, 1997, 137-142.

[8] Costa, L., Luda, M. P., Trossarelli, L., Brach del Prever, E. M., Crova, M. and Gallinaro, P., "Oxidation in Orthopaedic UHMWPE Sterilized by Gamma-Radiation and Ethylene Oxide," Biomaterials, 19, 7-9, 1998, 659-668.

[9] Devries, K. L., Smith, R. H. and Fanconi, B. M., "Free Radicals and New End Groups Resulting from Chain Scission: 1. γ-Irradiation of Polyethylene," Polymer, 21, 8, 1980, 949-956.

[10] Crowninshield, R. D. and Muratoglu, O. K., "How Have New Sterilization Techniques and New Forms of Polyethylene Influenced Wear in Total Joint Replacement?" Journal of the American Academy of Orthopaedic Surgeons, 16, suppl 1, 2008, s80-s85.

[11] Blanchet, T. A. and Burroughs, B. R., "Numerical Oxidation Model for Gamma Radiation-Sterilized UHMWPE: Consideration of Dose-Depth Profile," Journal of Biomedical Material Research, 58, 6, 2001, 684-693.

[12] Premnath, V., Harris, W. H., Jasty, M. and Merrill, E. W., "Gamma Sterilization of UHMWPE Articular Implants: an Analysis of the Oxidation Problem," Biomaterials, 17, 18, 1996, 1741-1753.

[13] O'Neill, P., Birkinshaw, C., Leahy, J. J., Buggy, M. and Ashida, T., "The Distribution of Oxidation Products in Irradiated Ultra-High Molecular Weight Polyethylene," Polymer Degradation and Stability, 49, 2, 1995, 239-244.

[14] Curier, B. H., John H, C., John P, C., Mayor, M. B. and Scott, R. D., "Shelf Life and In Vivo Duration; Impacts on Performance of Tibial Bearings," Clinical Orthopaedics and Related Research, 342, 1997, 111-122.

[15] Kyomoto, M., Ueno, M., Kim, S. C., Oonishi, H. and Oonishi, H., "Wear of "100 Mrad" Cross-Linked Polyethylene: Effects of Packaging After 30 Years Real-Time Shelf-Aging," Journal Biomaterial Science. Polymer Edition, 18, 1, 2007, 59-70.

[16] Fisher, J., Chan, K. and Hailey, J., "Preliminary Study of the Effect of Aging Following Irradiation on the Wear of Ultrahigh-Molecular-Weight Polyethylene," The Journal of Arthroplasty, 10, 5, 1995, 689-692.

[17] Toohey, K. S., Blanchet, T. A. and Heckelman, D. D., "Effect of Accelerated Aging Conditions on Resultant Depth-Dependent Oxidation and Wear Resistance of UHMWPE Joint Replacement Bearing Materials," Wear, 255, 7-12, 2003, 1076-1084.

[18] Mourad, A.-H. I., Fouad, H. and Elleithy, R., "Impact of Some Environmental Conditions on the Tensile, Creep-Recovery, Relaxation, Melting and Crystallinity Behaviour of UHMWPE-GUR 410-Medical Grade," Material and Design, 30, 10, 2009, 4112-4119.

[19] Alothman, O. Y., "Processing and Characterization of High Density Polyethylene/Ethylene Vinyl Acetate Blends with Different VA Contents," Advances in Materials Science and Engineering, 2012, 2012, 1-10.

[20] Sawae, Y., Yamamoto, A. and Murakami, T., "Influence of Protein and Lipid Concentration of the Test Lubricant on the Wear of Ultra High Molecular Weight Polyethylene," Tribology International, 41, 7, 2008, 648-656.

[21] Gilbert, J. L. and Merkhan, I., "Rate Effects on the Microindentation-Based Mechanical Properties of Oxidized Crosslinked, and Highly Crystalline Ultrahigh-Molecular-Weight Polyethylene," Journal of Biomedical Materials Research Part A, 71A, 3, 2004, 549-558.

[22] Wernlé, J. D. and Gilbert, J. L., "Micromechanics of Shelf-Aged and Retrieved UHMWPE Tibial Inserts: Indentation Testing, Oxidative Profiling, and Thickness Effects," Journal of Biomedical Materials Research Part B, Applied Biomaterial, 75, 1, 2005, 113-121.

[23] Watanabe, E., Suzuki, M., Nagata, K., Kaneeda, T., Harada, Y., Utsumi, M., Mori, A. and Moriya, H., "Oxidation-Induced Dynamic Changes in Morphology Reflected on Freeze-Fractured Surface of Gamma-Irradiated Ultra-High Molecular Weight Polyethylene Components," Journal of Biomedical Materials Research, 62, 4, 2002, 540-549.

# Wear Resistance of the Biocompatible Phospholipid Polymer-Grafted Highly Cross-Linked Polyethylene Liner Against Larger Femoral Head

Toru Moro,[1,2] Yoshio Takatori,[1,2] Masayuki Kyomoto,[1,3,4] Kazuhiko Ishihara,[3] Hiroshi Kawaguchi,[5] Masami Hashimoto,[6] Takeyuki Tanaka,[2] Hirofumi Oshima,[2] Sakae Tanaka[2]

[1]Division of Science for Joint Reconstruction, Graduate School of Medicine, The University of Tokyo, 7-3-1 Hongo, Bunkyo-ku, Tokyo 113-8655, Japan, [2]Sensory & Motor System Medicine, Faculty of Medicine, The University of Tokyo, 7-3-1 Hongo, Bunkyo-ku, Tokyo 113-8655, Japan, [3]Department of Materials Engineering, School of Engineering, The University of Tokyo, 7-3-1 Hongo, Bunkyo-ku, Tokyo 113-8656, Japan, [4]Research Department, KYOCERA Medical Corporation, 3-3-31 Miyahara, Yodogawa-ku, Osaka 532-0003, Japan, [5]Japan Community Health care Organization, Tokyo Shinjuku Medical Center, Spine Center, 5-1 Tsukudo, Shinjuku-ku, Tokyo 162-8543, Japan, [6]Materials Research and Development Laboratory, Japan Fine Ceramics Center, 2-4-1 Mutsuno, Atsuta-ku, Nagoya 456-8587, Japan

*Received 19 October 2014; accepted 13 February 2015*
*Published online in Wiley Online Library (wileyonlinelibrary.com). DOI 10.1002/jor.22868*

**ABSTRACT:** The use of larger femoral heads to prevent the dislocation of artificial hip joints has recently become more common. However, concerns about the subsequent use of thinner polyethylene liners and their effects on wear rate have arisen. Previously, we prepared and evaluated the biological and mechanical effects of a novel highly cross-linked polyethylene (CLPE) liner with a nanometer-scaled graft layer of poly(2-methacryloyloxyethyl phosphorylcholine) (PMPC). Our findings showed that the PMPC-grafted particles were biologically inert and caused no subsequent bone resorptive responses and that the PMPC-grafting markedly decreased wear in a hip joint simulator. However, the metal or ceramic femoral heads used in this previous study had a diameter of 26 mm. Here, we investigated the wear-resistance of the PMPC-grafted CLPE liner with a 40-mm femoral head during $10 \times 10^6$ cycles of loading in the hip joint simulator. The results provide preliminary evidence that the grafting markedly decreased gravimetric wear rate and the volume of wear particles, even when coupled with larger femoral heads. Thus, we believe the PMPC-grafting will prolong artificial hip joint longevity both by preventing aseptic loosening and by improving the stability of articular surface. © 2015 Orthopaedic Research Society. Published by Wiley Periodicals, Inc. J Orthop Res

**Keywords:** artificial hip joint; total hip arthroplasty; periprosthetic osteolysis; aseptic loosening

In addition to aseptic loosening, dislocation is one of the most common causes of revision of total hip arthroplasty (THA).[1] The dislocation rates are reported to range from less than 1% to 5% after primary THA[2,3] and up to 5–15% after revision THA.[4] Most dislocations occur in the first 6 weeks after surgery, and about one-third become recurrent and require revision surgery.[5,6]

Although dislocation is a multifactorial complication dependent on various factors (e.g., implant malpositioning),[7] larger femoral heads provide mechanical advantages that can improve stability of the articular surface of THA. The head/neck ratio is increased with the use of larger femoral heads, which can prevent impingement between the trunnion and the acetabular component.[8] Decreased impingement, combined with the increased amount of displacement required before the head dislocates (jump distance), also reduces the dislocation risk.[8] Hence, the use of larger femoral heads for improving the stability of the THA has recently become more common,[2,9] and multiple studies have demonstrated larger femoral heads reduce dislocation rates clinically.[10,11] However, larger femoral heads (e.g., 36 or 40 mm in diameter) have an increased sliding distance and velocity per step between bearing surfaces of the THA, leading to an increased wear rate as compared to smaller femoral heads.[9] Moreover, a larger femoral head requires a thinner polyethylene (PE) liner for retaining acetabular bone, which can produce higher contact stresses, possibly accelerating wear and/or fracture of the liner,[12] and, therefore, may increase the production of wear particles, consequently resulting in osteoclastogenesis, bone resorption, and periprosthetic osteolysis.[13] Thus, larger femoral heads may increase the risk for aseptic loosening, a factor closely related to the rate of PE wear.[14] Therefore, new technologies that decrease not only the dislocation rate but also the production of wear particles are needed.

For preventing periprosthetic osteolysis and aseptic loosening, we developed a novel bearing surface with cartilage-mimicking hydrogel structures. Recent studies have shown the human articular cartilage surface is covered with a nanometer-scaled phospholipid layer that functions to protect the articulating surface from mechanical wear, to provide hydrophilicity, and to act as a boundary lubricant.[15] Thus, we grafted the biocompatible phospholipid polymer, poly(2-methacryloyloxyethyl phosphorylcholine) (PMPC), onto a highly cross-linked PE (CLPE). The nanometer-scale layer of PMPC (100–150 nm in thickness) with the cartilage-mimicking hydrogel structures provides

Conflicts of interest: The sponsors had no role in the study design, data collection, data analysis, data interpretation, or writing of the manuscript. Co-author (K.M.) is employed by KYOCERA Medical Corporation.
Grant sponsor: Health and Welfare Research Grant; Grant numbers: H23-007, H24-001, H26-006; Grant sponsor: Japanese Ministry of Health, Labour and Welfare.
*Correspondence to*: Toru Moro (T: +81-3-3815-5411 ext. 30474; F: +81-3-3818-4082; E-mail: moro-ort@h.u-tokyo.ac.jp)

hydrophilicity and lubricity mimicking the articular cartilage surface without affecting the CLPE substrate physical or mechanical properties.[16] The PMPC grafting on the CLPE surface was shown to increase the lubrication to levels matching articular cartilage under physiological conditions.[17] Our recent study on the mechanical effects of PMPC grafting revealed that it markedly decreased wear particle production and that the effect of PMPC grafting was maintained through 70 million cycles in a hip joint simulator.[18] The PMPC-grafted particles were also shown to be biologically inert and not to result in bone resorptive responses.[19] Based on multicenter clinical trials of the PMPC-grafted CLPE (PMPC-CLPE) acetabular liners performed from 2007 in Japan (UMIN00003681), the liners were reported as a safe implant option for hip replacement surgery after a 3-year clinical use.[20] In this cohort study of 76 joints, the mean wear rate was 0.002 mm/year, representing about an 80–97% reduction as compared to other CLPE liners.[21–26] At the time this article was written, neither periprosthetic osteolysis nor a requirement for revision surgery had been observed after a minimum of 5 years and a maximum of 7 years of follow-up.

However, metal or ceramic femoral heads with a diameter of 22 or 26 mm were used in our previous studies.[17–19] The present study investigated the wear resistance of the PMPC-grafted CLPE liner with a 40-mm femoral head during $10 \times 10^6$ cycles in a hip joint simulator test.

## METHODS

### Hip Joint Simulator

Acetabular liners were produced from GUR1020 ultra-high molecular weight polyethylene bar stock irradiated at 50-kGy for cross-linking (K-MAX® CLQC, KYOCERA Medical Corporation, Osaka, Japan), and surface modified by using a photoinduced graft polymerization of MPC (NOF Co. Ltd., Tokyo, Japan), as previously reported.[17,19] All liners were subsequently sterilized by 25-kGy gamma-ray irradiation under $N_2$ gas. Cobalt–chromium–molybdenum (CoCrMo) alloy femoral heads (26 or 40 mm in diameter) (K-MAX® HH-02, KYOCERA Medical Corporation) were used in this study. The thickness of the acetabular liner was 10 and 6 mm in the 26-mm and 40-mm femoral head groups, respectively. Under the conditions recommended by ISO 14242-3, CLPE ($N = 3$) or PMPC-CLPE ($N = 3$) acetabular liners were tested against 26-mm or 40-mm CoCrMo alloy femoral heads on a 12-station hip simulator (MTS Systems Corp., Eden Prairie, MN) at 1 Hz; 700 ml of 25% (v/v) bovine serum was used as the lubricant and was replaced every $0.5 \times 10^6$ cycles. Sodium azide (10 mg/L) and ethylenediaminetetraacetic acid (20 mM) were added for preventing microbial contamination and minimizing calcium phosphate formation on the implant surface. A physiological loading curve (Paul-type) with double peaks at 1793- and 2744-N loads with a multidirectional (biaxial and orbital) motion were used as gait cycles.[27] The simulator was run up to $10 \times 10^6$ cycles. Wear was determined by gravimetric measurement of the liners at intervals of $0.5 \times 10^6$ cycles. Because the liners absorbed fluids (e.g., water, lipids) while soaking in the lubricant, wear measurements were corrected by load-soak controls ($N = 2$), according to ISO 14242-2. Weight loss in the tested liners was corrected by subtracting the weight gain of the load-soak controls. Wear rates were determined by linear regression and were estimated at intervals of $0–10 \times 10^6$ cycles.

### Analyses of Joint Surfaces

After $10 \times 10^6$ cycles, morphological changes in the liner surface were measured using a 3-dimensional (3D) coordinate measuring instrument (BHN-305, Mitsutoyo Corp., Kawasaki, Japan) and reconstructed using 3D modeling software (Imageware, Siemens PLM Software, Inc., Plano, TX). For evaluating wear-induced alterations in surface morphology, the liner surface was analyzed using a confocal scanning laser microscope (OLS1200, Olympus, Tokyo, Japan).

### Analyses of Wear Particles

After isolation from the bovine serum solution,[28] wear particles were analyzed according to the ASTM F1877-05 standard and digitally imaged on a field emission scanning electron microscope (JSM-633OF, JEOL Datum Co. Ltd., Tokyo, Japan). An image-processing program (Scion Image, Scion Corp., Frederick, MD) was used to determine the volume of wear particles per $10^6$ cycles.[29] Two size descriptors (equivalent circle diameter [ECD], diameter) and two shape descriptors (aspect ratio, roundness) were used to define each wear particle, according to ASTM F1877-98.[18] Each parameter was defined as follows: ECD was defined as the diameter of a circle with an area equivalent to that of one wear particle. The diameter was defined using the maximum dimensions as determined by the SEM analysis. The aspect ratio was defined as the ratio of the major diameter to the minor diameter. It should be noted that the major diameter represented the longest straight line that could be drawn between any two points on the outline. On the other hand, the minor diameter represented the longest line perpendicular to the major diameter. Roundness was a measure of how closely a wear particle resembled a circle; its values ranged from 0 to 1, with a perfect circle having a roundness value of 1.

### Statistical Analysis

Differences between wear rates and between the size and shape descriptors of particles were accessed for significance by the Student's $t$-test. All statistical analyses were conducted using add-in software (Statcel 2; OMS Publishing, Inc., Tokorozawa, Japan) on Microsoft Excel.

## RESULTS

We initially estimated the weight gain of the load-soak control liners. The mean weight gain in the load-soak controls of the untreated CLPE liners was 3.87 and 4.20 mg for the 26- and 40-mm CoCrMo alloy femoral heads, respectively. Similarly, the mean weight gain in the load-soak controls of the PMPC-CLPE liners was 3.74 and 3.28 mg for the 26- and 40-mm CoCrMo alloy femoral heads, respectively. For the 26-mm CoCrMo alloy femoral heads, the load-soak control liners showed comparable weight gains during $10 \times 10^6$ cycles, irrespective of the PMPC grafting. For the 40-mm CoCrMo alloy femoral heads, the